International Journal of Innovative Computing, Information and Control
Volume **22**, Number **1**, February **2026**

ICIC International ©2026 ISSN 1349-4198
pp. **65–78**

RESEARCH ON DYNAMICS OF CRACKED GEAR PAIR CONSIDERING THE LUBRICATION EFFECT AND LOAD-DEPENDENT MESH STIFFNESS

Zufeng Li[1,2,*] and Jiarui Fan[2]

[1]National Research Base of Intelligent Manufacturing Service
[2]School of Mechanical Engineering
Chongqing Technology and Business University
No. 19, Xuefu Avenue, Nan'an District, Chongqing 400067, P. R. China
fanjiarui@ctbu.edu.cn
*Corresponding author: zufengli@ctbu.edu.cn

Received April 2025; revised July 2025

Abstract. *In the actual gear system, it is possible to produce root cracks of gear working under lubrication condition. The mesh stiffness and lubrication performance changes obviously as the decrease of load bearing capacity for the crack tooth pair, which affects eventually the dynamic characteristics of gear system. An enhanced tribo-dynamic model of the gear pair is proposed, incorporating gear crack failure and lubrication performance. This model couples the elastohydrodynamic lubrication and lateral-torsional dynamics. Utilizing deformation coordination condition, the influence of tooth crack on both total mesh stiffness and lubrication performance is investigated. The results show that the amplitude of vibration displacement grows obviously due to the impact caused by the crack tooth pair engaging in contact, and some frequency clusters are generated near resonance frequencies. By comparing lubrication and dry contact conditions, the effectiveness of RMS and kurtosis values in tracking crack severity progression is proved. It is found that condition indicators with the lubrication effect increase significantly with the crack in the off-line-of-action direction.*

Keywords: Gear system, Mesh stiffness, Lubrication performance, Tooth crack severity, Dynamic characteristics

1. **Introduction.** Gearbox is one of the most critical parts of industrial systems, because it is widely used to transfer power and change speed. Because of the complicated and changeable working conditions, gear system has the potential for various failures, which can cause catastrophic accidents and major economic losses. Therefore, the early detection of gearbox failure is very important. Due to the complicated structure of the gear system and complex interaction between the components, corresponding vibration mechanism of the gear system with failures is still unclear. Crack failure at gear root is typically caused by surface fatigue resulting from alternating loads during gear operation. These cracks generally spread along the stress concentration area at the tooth root, and eventually lead to the failure.

For understanding vibration mechanisms with fault characteristics, a dynamic model of gear system with faults has been an interesting research topic [1]. In addition, a well-validated dynamic model, verified by test results, provides an excellent signal source for validating fault detection and diagnosis methods. Meanwhile, these signals can be used to feed or train artificial intelligence fault diagnosis algorithms, and can also be used as a test set and verification set for training gearbox faults. However, most existing studies

DOI: 10.24507/ijicic.22.01.65

primarily focus on obtaining time-varying mesh stiffness (TVMS) of cracked gear pair under quasi-static condition, which is insufficient to adequately reveal the relationship between TVMS and load distribution factor (LDF) during actual operational condition. Therefore, the modeling process of tribo-dynamic behaviors for the cracked gear pair is very complicated.

In summary, it is necessary to take many factors into dynamic model, such as mesh stiffness, lubrication factor, surface friction and crack fault. The purpose of tribo-dynamic research for cracked gear pair is to deeply understand dynamic responses under different crack fault severities, so as to provide theoretical basis for fault diagnosis.

This paper is organized as follows. Section 2 describes the current research status of mesh stiffness and tribo-dynamic characteristics of crack gear pairs, and proposes a dynamic response analysis scheme considering crack fault and lubrication effects. Section 3 establishes a tribo-dynamic coupled model of the crack gear pair. In Section 4, simulation analysis is used to verify the accuracy of the proposed model, and discusses the variation of dynamic responses with crack fault severity. Finally, Section 5 is the conclusions.

2. **Related Work.** In helicopter, wind turbine, ships and other industrial equipment, gearbox failures may cause catastrophic damage, resulting in significant economic losses and even casualties. Various faults may occur in gearboxes under the action of alternating loads, such as tooth crack and pitting [2]. Among them, tooth crack is a more common failure mode. When the crack tooth pair engages, there is an obvious reduction of total TVMS for the gear pair. And TVMS is one of the main parametric excitations and affects the system vibration characteristics [3]. For system condition monitoring and fault identification, it is very necessary to study impact of crack fault on gear system dynamics.

For cracked gear system, fault identification generally focuses on the mesh stiffness with faults and dynamic characteristics from vibration analysis [4]. Wu et al. [5] used multiple condition indicators to study the different crack severity on the dynamic responses of the gear pair, such as root mean square (RMS) and kurtosis values. Chen et al. [6,7] analyzed the effect of tooth crack on tooth stiffness and fillet foundation stiffness, and then they studied the influence of tooth crack on dynamic behaviors with different crack depths and lengths. Ma and Chen [8] studied the effect of local defects on the vibration behaviors by incorporating tooth crack into the dynamic model. Meng et al. [9] calculated time-varying mesh stiffness with different crack lengths, and established a six degree-of-freedoms dynamic model taking mesh stiffness and friction force into account. Wan et al. [10] proposed a modified mesh stiffness model with crack fault, and then used a lateral and torsional coupled dynamic model to simulate the effect of mesh stiffness and bearing stiffness on vibration responses. To simplify, most of the above dynamic models focus on the influence of crack fault on the mesh stiffness, and then affect the vibration responses of gear system.

Some research works analyzed the interaction between lubrication performance and dynamic characteristics for the gearbox through contact parameters, such as tooth surface friction, oil film stiffness, oil film damping and time-varying backlash. He et al. [11] established multi-degree-of-freedom dynamic model with friction excitation, which compared the effects of four different friction formulas on the dynamic responses. Li and Kahraman [12] proposed a tribo-dynamic model of the spur gear pair, which considered the coupling interation between friction force, tangential oil film damping and dynamic mesh force. Zhou et al. [13,14] calculated oil film stiffness and damping through the elastohydrodynamic lubrication (EHL) model, and then evaluated the impact of oil film stiffness and damping on vibration responses. Considering tooth clearance, Zhou et al. [15,16] established a multi-mass transmission system of wind turbine, and discussed the nonlinear characteristics of clearance and the principle of nonlinear vibration. Chen et al. [17] incorporated lubricant film into backlash, resulting in the reduction of backlash. They investigated the influence of lubricant viscosity on the dynamic responses, showing that vibration amplitudes decrease with the lubricant viscosity along off-line-of-action (OLOA) direction.

Furthermore, lubrication effect and crack fault were considered simultaneously in few gear dynamics studies. Zhao et al. [18] systematically analyzed the impact of tooth crack fault on lubrication performance, subsequently exploring the combined effect of both lubrication performance and crack propagation on the vibration responses. Yang et al. [19] considered the combined mesh stiffness and damping incorporating both lubrication effect and crack fault, and then investigated gear dynamic responses. However, lubrication characteristics and mesh stiffness in above researches were obtained under quasi-static condition.

Some researches has mainly focused on the calculation of lubrication performance and equivalent mesh stiffness for the gear pair under dynamic condition. Cao et al. [20] proposed a nonlinear relationship between the mesh stiffness and mesh force, and then jointly solved the dynamic mesh stiffness and dynamic responses of gear system. Li et al. [21] established a tribo-dynamic model for a gear pair, and lubrication characteristics and mesh stiffness were obtained under dynamic mesh force. Wang et al. [22] studied the effect of spalling fault on lubrication characteristics and dynamic responses for gear system.

In fact, gear crack fault may appear even in transmission system operating under lubrication condition. As seen from the above literature, some studies analyzed the influence of mesh stiffness and lubrication characteristics over dynamic mesh force on system responses for the healthy gear pair [12,21], and some research investigated lubrication characteristics over static load and crack fault acting on the system responses [18,19]. To address this, a more comprehensive tribo-dynamic model must be developed for the cracked gear system, incorporating both tooth crack and lubrication performance. Crucially, the calculation of lubrication contact parameters must account for dynamic load fluctuation and load distribution within the double-tooth-pair-contact duration. By using the established tribo-dynamic model, the influence of crack fault and lubrication performance on the gear system dynamic responses is investigated, and change of condition indicators with the crack severity is discussed.

3. Construction of Tribo-Dynamic Coupled Model for the Cracked Gear.

3.1. Tribo-dynamic coupled model. The lumped parameter model proposed in [12] is employed in analyzing dynamic characteristics of a gear system, which considers the interaction between the tribological properties and dynamic responses. It is easy to see that the gear system consists of a pinion and a gear, as shown in Figure 1.

The gear is assumed to be a rigid body with base circle radius r_{bi}, mass M_i and moment of inertia J_i. Each gear has 3 degree-of-freedoms (DOFs), namely the torsional freedom θ_i, translational freedom along the line-of-action (LOA) z_i and translational freedom along the OLOA x_i. The input torque T_p is applied to the pinion and output torque T_g is applied to the gear, satisfying $T_p = T_g r_{bp}/r_{bg}$. According to the lumped parameter method, a six-DOFs dynamic equation for the gear pair is constructed as

$$J_p\ddot{\theta}_p(t) + c_{tp}\dot{\theta}_p(t) + r_{bp}F_{dm}(t) = T_p + \sum_{j=1}^{n=1,2} F_{fpj}(t)R_{pj}(t) \tag{1a}$$

$$J_g\ddot{\theta}_g(t) + c_{tg}\dot{\theta}_g(t) - r_{bg}F_{dm}(t) = -T_g - \sum_{j=1}^{n=1,2} F_{fgj}(t)R_{gj}(t) \tag{1b}$$

$$M_p\ddot{z}_p(t) + c_{zp}\dot{z}_p(t) + k_{zp}z_p(t) = -F_{dm}(t) \tag{1c}$$

$$M_g\ddot{z}_g(t) + c_{zg}\dot{z}_g(t) + k_{zg}z_g(t) = F_{dm}(t) \tag{1d}$$

$$M_p\ddot{x}_p(t) + c_{xp}\dot{x}_p(t) + k_{xp}x_p(t) = \sum_{j=1}^{n=1,2} F_{fpj}(t) \tag{1e}$$

$$M_g\ddot{x}_g(t) + c_{xg}\dot{x}_g(t) + k_{xg}x_g(t) = -\sum_{j=1}^{n=1,2} F_{fgj}(t) \tag{1f}$$

where, the subscripts p and g represent the pinion and gear, respectively; R_p and R_g are arms of friction force; F_{fpj} and F_{fgj} are the friction force of the jth tooth pair; if $n = 1$, it means in single-tooth-contact (STC) region; if $n = 2$, it means in double-tooth-contact (DTC) region; k_{xp}, k_{xg}, c_{xp} and c_{xg} are support stiffness and damping of bearings in OLOA, respectively; k_{zp}, k_{zg}, c_{zp} and c_{zg} are support stiffness and damping of bearings in LOA, respectively; c_{tp} and c_{tg} are torsional damping; F_{dm} is dynamic mesh force.

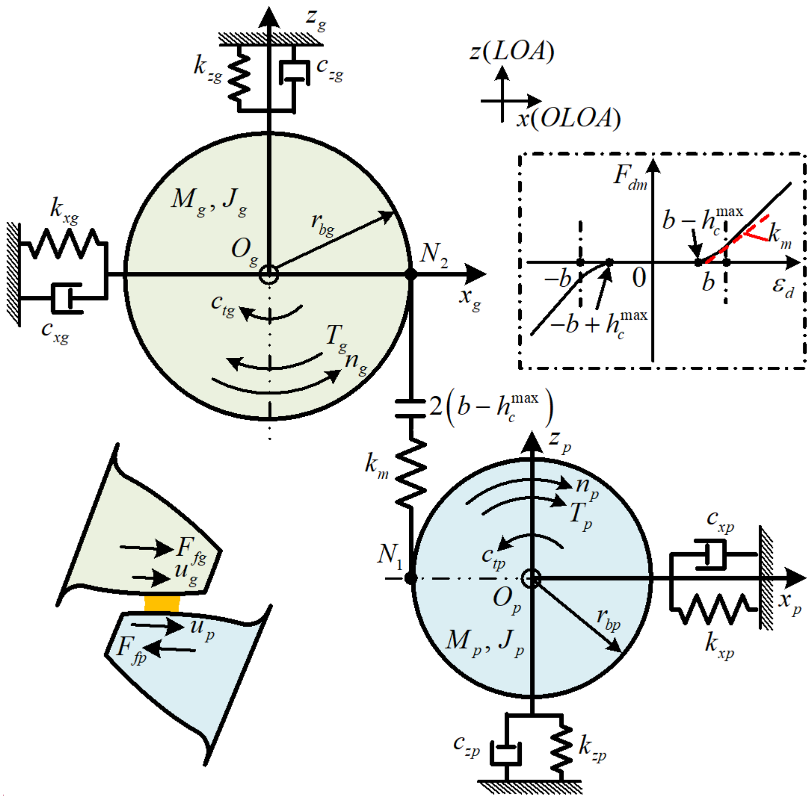

FIGURE 1. A tribo-dynamic model for the gear system

Under lubrication condition, the nonlinear deformation function of a gear pair is expressed by a piecewise form, as follows [21]:

$$\epsilon(t) = \begin{cases} \varepsilon_d(t) - \left(b - h_c^{\max}(t)\right); & \varepsilon_d(t) > b - h_c^{\max}(t) \\ 0; & |\varepsilon_d(t)| \le b - h_c^{\max}(t) \\ \varepsilon_d(t) + \left(b - h_c^{\max}(t)\right); & \varepsilon_d(t) < -(b - h_c^{\max}(t)) \end{cases} \tag{2}$$

where, $\varepsilon_d(t) = r_{bp}\theta_p(t) - r_{bg}\theta_g(t) + z_p(t) - z_g(t)$ is the dynamic transmission error (DTE); b is the backlash; $h_c^{\max}(t)$ is the upper limit of center oil film thickness generating contact force.

Based on the time domain data, some signal indicators are widely used in gear transmission fault detection. Thereinto, the RMS is often used to analyze the overall vibration level, and the kurtosis is suitable to describe the impulse signal caused by defected components. The RMS and kurtosis are respectively [5]

$$\mathrm{RMS} = \sqrt{1/N \sum_{n=1}^{N} \left(\varepsilon_d(n) - \overline{\varepsilon_d}\right)^2} \tag{3}$$

$$\mathrm{KUR} = \frac{1/N \sum_{n=1}^{N} \left(\varepsilon_d(n) - \overline{\varepsilon_d}\right)^4}{\left[1/N \sum_{n=1}^{N} \left(\varepsilon_d(n) - \overline{\varepsilon_d}\right)^2\right]^2} \tag{4}$$

where, N denotes the number of data points in the sampled signal; $\varepsilon_d(n)$ is the value of the nth point; $\overline{\varepsilon_d}$ is the mean value of DTE.

3.2. **Mesh stiffness and load distribution models.** For a cracked gear pair, mesh stiffness is calculated by potential energy method [23]. The crack propagation is assumed to be a straight, and limit line between the end point of crack and tip of addendum circle can be supposed to a parabola. Considering the impact of tooth root crack fault on the bending, shear, fillet foundation stiffness, an improved stiffness model of the cracked gear pair is proposed [7]. A mesh stiffness model is proposed for the gear pair with a root crack on pinion, and geometric parameters of tooth and fillet foundation are shown in Figure 2.

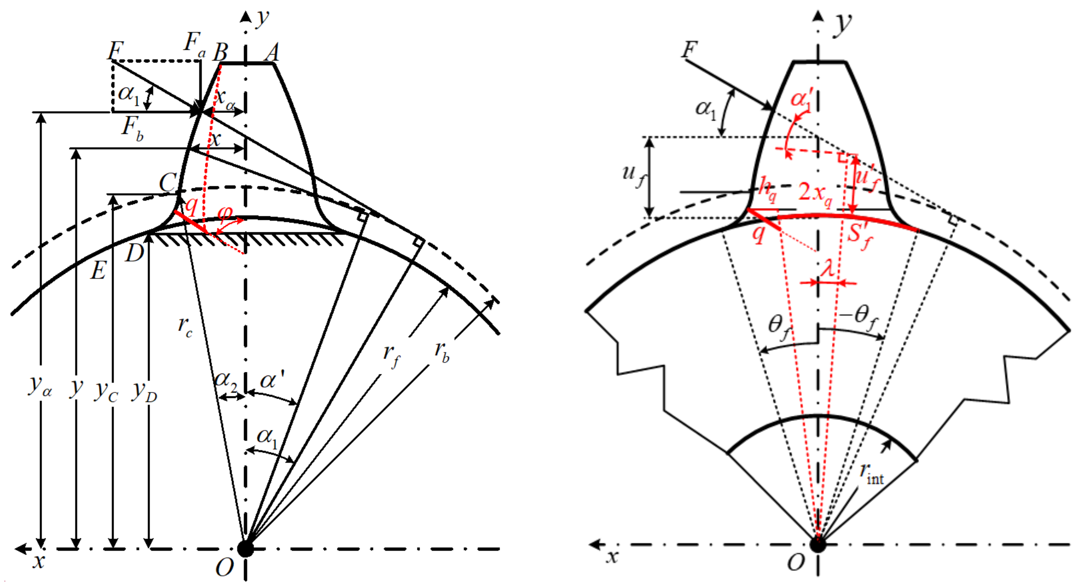

(a) Tooth deformation (b) Fillet-foundation deformation

FIGURE 2. Geometric parameters of the cracked gear

The equations of the bending stiffness k_b, axial compressive stiffness k_a, shear stiffness k_s and fillet foundation stiffness k_f are expressed as

$$\frac{1}{k_b} = \int_{y_D}^{y_C} \frac{\left[(y_\alpha - y_1)\cos\alpha_1 - x_1 \sin\alpha_1\right]^2}{EI_{y1}} dy_1$$

$$+\int_{y_C}^{y_\alpha}\frac{[(y_\alpha-y_2)\cos\alpha_1-x_1\sin\alpha_1]^2}{EI_{y2}}dy_2 \tag{5}$$

$$\frac{1}{k_a}=\int_{y_D}^{y_C}\frac{(\sin\alpha_1)^2}{EA_{y1}}dy_1+\int_{y_C}^{y_\alpha}\frac{(\sin\alpha_1)^2}{EA_{y2}}dy_2 \tag{6}$$

$$\frac{1}{k_s}=\int_{y_D}^{y_C}\frac{1.2(1+v)(\cos\alpha_1)^2}{EA_{y1}}dy_1+\int_{y_C}^{y_\alpha}\frac{1.2(1+v)(\cos\alpha_1)^2}{EA_{y2}}dy_2 \tag{7}$$

$$\frac{1}{k_f}=\frac{\cos^2\alpha_1'}{EL}\left\{L^*\left(\frac{u_f'}{S_f'}\right)^2+M^*\left(\frac{u_f'}{S_f'}\right)+P^*\left(1+Q^*\tan^2\alpha_1'\right)\right\} \tag{8}$$

where, I and A represent the moment of inertia and area of cross section, respectively; E is elastic modulus; v denotes Possion's ratio; L is tooth width; α_1 is the actual mesh angle; parameters L^*, M^*, P^* and Q^* are described in [23], and parameters of α_1', u_f' and S_f' related to the load bearing region of the crack gear tooth can be detailed in [7].

Regardless of dry or lubrication contact conditions, rigid body displacement h_0 is used to indicate the ability of tooth contact pair to resist deformation, which rises nonlinearly with the increase of tooth force. Therefore, contact stiffness is derived from tooth force and rigid body displacement by partial differentiation, which is presented as [24]

$$\frac{1}{k_c}=\frac{\partial h_0}{\partial F} \tag{9}$$

Including force-dependent effect, equivalent mesh stiffness of a tooth pair is written as

$$k_e=1/(1/k_{li}+1/k_c) \tag{10}$$

where, $k_{li}=1/(1/k_{bp}+1/k_{ap}+1/k_{sp}+1/k_{fp}+1/k_{fg}+1/k_{sg}+1/k_{ag}+1/k_{bg})$ is the stiffness component independent of the force.

When the load is transferred, there are one or two tooth pairs in contact. Therefore, the total mesh stiffness of a gear pair can be described as

$$k_m=\sum_{j=1}^{n}k_{ej},\ (n=1\text{ or }2) \tag{11}$$

It is worth noting that the mesh force is supported by one or two tooth pairs in a mesh cycle (T_m). The load is shared by two parallel springs with different stiffness in DTC region (T_{dm}), so the load distribution factor is not uniform, especially cracked gear pair. According to the deformation coordination condition, the relationship between mesh deformation and tooth force between tooth pair 1 and tooth pair 2 can be expressed as

$$\begin{cases}\delta_{e1}=F_1(t)/k_{li,1}+h_{0,1}(F_1,t)\\ \delta_{e2}=F_2(t)/k_{li,2}+h_{0,2}(F_2,t)\end{cases} \tag{12}$$

Therefore, the load distribution factors γ_1 and γ_2 for tooth pair 1 and tooth pair 2 are calculated as

$$\begin{cases}\gamma_1=F_1/F_m\\ \gamma_2=F_2/F_m\\ F_1+F_2=F_m\end{cases} \tag{13}$$

It is pointed out that F_m is the static mesh force under quasi-static condition or dynamic mesh force under tribo-dynamic condition.

3.3. **Lubrication model.** The lubricant is filled between the two engaged tooth surfaces due to the entraining effect, which plays the role of support and lubrication. Firstly, lubrication performance can be calculated from EHL model of infinite line contact, and then the impact of oil film stiffness and damping effect on the dynamic response can be analyzed for gear transmission system. The Reynolds equation is adopted to depict fluid behavior, which is given as [25]

$$\frac{\partial}{\partial x}\left[\left(\frac{\rho}{\eta}\right)_e h(x,t)^3\frac{\partial p(x,t)}{\partial x}\right]=12u_r\frac{\partial(\rho^* h(x,t))}{\partial x}+12\frac{\partial(\rho_e h(x,t))}{\partial t} \tag{14}$$

where, p and h denote the film pressure and thickness, respectively; $(\rho/\eta)_e$, ρ^*, and ρ_e represent the characteristic parameters of the fluid; x is the rolling direction; t is the time.

Considering elastic deformation of two contact bodies, film thickness is

$$h(x,t)=-h_0(t)+\frac{x^2}{2R(t)}-\frac{4}{\pi E_0}\int_{x_{in}}^{x_{out}}\ln\left|\frac{x-x'}{x_0}\right|p(x',t)dx' \tag{15}$$

where, R is the equivalent redius; E_0 is the equivalent elastic modulus.

In contact area, the force obtained by integrating on the film pressure is equal to the load acted on the tooth pair. So the load balance equation is

$$\int_{x_{in}}^{x_{out}} p(x,t)dx=w(t) \tag{16}$$

where, $w=F/L$ is tooth force per unit length; F is static or dynamic tooth force.

Assume that shear stress changes linearly along the film thickness, which can be expressed as

$$\tau(x,z,t)=\frac{\eta_e}{h(x,t)}(u_g(t)-u_p(t))+\left[z-\frac{\eta_e}{\eta_e'}h(x,t)\right]\frac{\partial p(x,t)}{\partial x} \tag{17}$$

where, u_p and u_g are surface velocities of the tooth pair, respectively.

The surface friction coefficient is computed by integrating the shear stress, as follows:

$$\mu(t)=\left|\int_{x_{in}}^{x_{out}}\tau dx\right|\Big/w(t) \tag{18}$$

Other governing equations of the EHL model are described in detail in [25].

3.4. **Numerical scheme.** To ensure the calculation accuracy of the pressure, tooth force and mesh deformation, the convergence criteria are

$$\begin{cases}\varepsilon_p=\left(\sum|p-\tilde{p}|\right)\Big/\left(\sum|p|\right)\le 10^{-5}\\ \varepsilon_w=\left(\sum|p|\right)\Big/w\le 10^{-5}\\ \varepsilon_\delta=|\delta_{e1}-\delta_{e2}|/|b|\le 10^{-4}\end{cases} \tag{19}$$

where, $\tilde{p}$ is the pressure of the previous iteration loop.

Numerical scheme of a tribo-dynamic model for cracked gear pair is shown in Figure 3. The main steps are as follows. 1) Utilizing the potential energy method, the bending, shear, axial compressive and fillet foundation stiffness are calculated. 2) The EHL model of line contact is solved by chasing method and DC-FFT, obtaining film pressure, thickness, rigid body displacement and shear stress. 3) Combined with lubrication performances, total mesh stiffness, time-varying backlash, and friction force/moment are calculated and substituted into the dynamic model. And vibration responses and dynamic characteristics are obtained by the Newmark method. 4) If relative errors of pressure and tooth force meet accuracy requirements, mesh position (DTC or STC) is determined; if not, EHL model is recalculated after updating the rigid body displacement and pressure. 5) Mesh

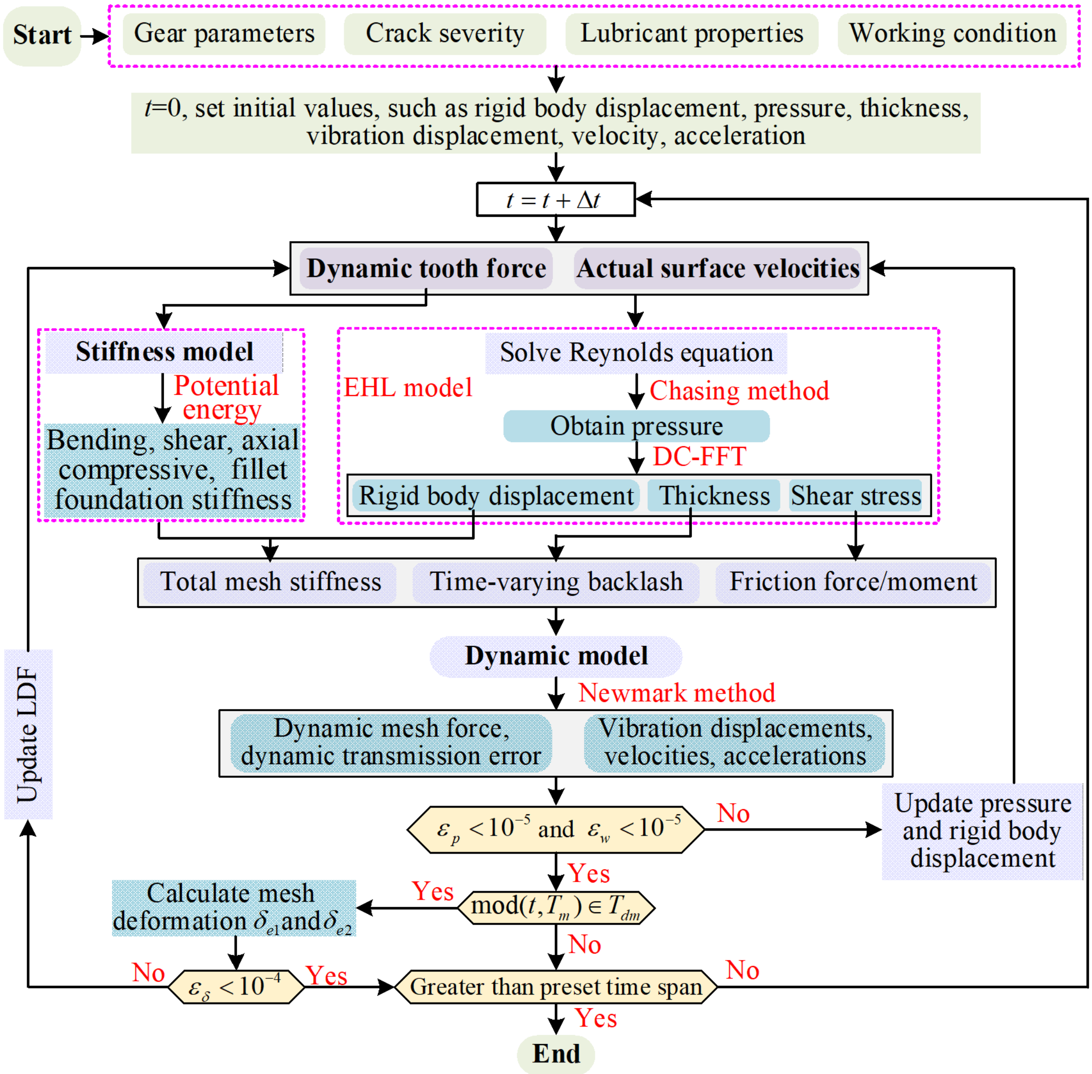

FIGURE 3. Numerical scheme

deformations are calculated in DTC region, and LDF is updated by deformation coordination condition until the convergence accuracy is satisfied. Particularly, this step is not executed in STC region. 6) If computation time has not exceeded the preset time span, next time step is calculated.

4. **Results and Discussions.** Through numerical simulation, dynamic responses are studied by considering the gear lubrication performance and root crack severity. Condition indicators, namely RMS and kurtosis values, are used to reveal the variation of dynamic responses with the crack severity. The main parameters of the gear pair are listed in [21], and an M1 lubricant is selected for lubrication analysis [18], as shown in Table 1. Moreover, it is assumed that the root crack angle φ is $\pi/3$. And the tooth root crack propagation severity is preset to $0 \sim 70\%$, which is the ratio of actual crack depth to theoretical maximum value across tooth thickness.

At input speed 2400 rpm away from the resonance region, the DTE predicted from three dynamic models for a healthy gear pair is compared in Figure 4(a). Under the dry contact condition, contact stiffnesses of each tooth pair from traditional model and dry-dynamic coupled (DDC) model are computed under the static tooth force and dynamic tooth force, respectively. Whereas, a tribo-dynamic coupled (TDC) model adopts total mesh stiffness

Table 1. Main parameters of the gear pair and M1 lubricant

Parameters	Values	Parameters	Values
Number of teeth Z_p/Z_g	42/86	Backlash b (μm)	120
Normal module m (mm)	2.5	Elastic modulus E_p/E_g (GPa)	210/210
Pressure angle α (deg)	20	Poisson's ratio v_p/v_g	0.3/0.3
Tooth width L (mm)	30	Viscosity η_0 (Pa·s)	0.1135
Mass M_p/M_g (kg)	1.7/7.2	Density ρ_0 (kg/m^3)	908
Moment of inertia J_p/J_g (kg·m^2)	2.69×10^{-3}/ 4.77×10^{-4}	Pressure-viscosity coefficient α (GPa^{-1})	19.95

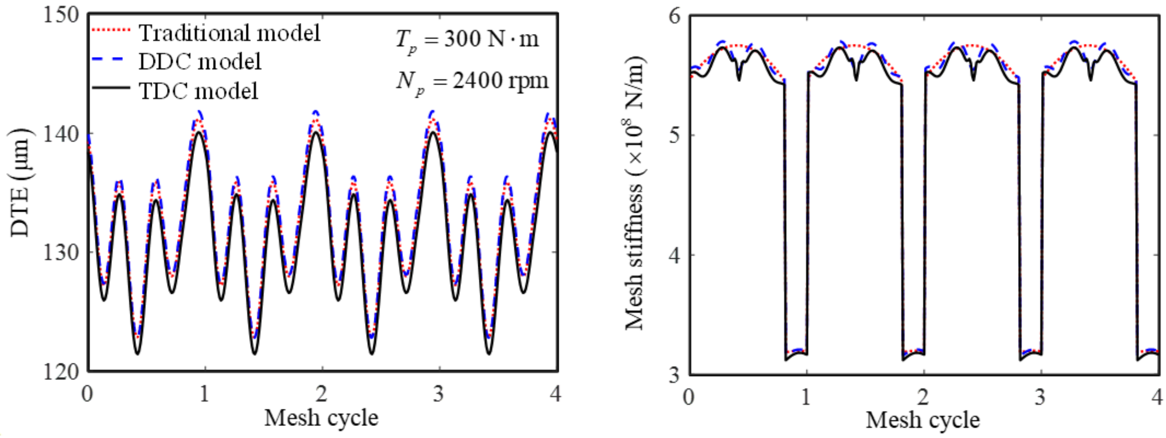

(a) DTE (b) Mesh stiffness

Figure 4. Comparison of DTE and mesh stiffness obtained from different dynamic models

including local contact stiffness, which is calculated by the dynamic tooth force under lubrication condition. The fluctuation curves of DTE predicted by three models are similar, while those amplitudes have a slight change. The lubrication effect is introduced into the TDC model, which changes the mesh excitations of the gear pair, such as friction force, oil film stiffness, oil film damping and time-varying backlash. Compared with the other two models, a downward trend in DTE obtained from TDC model verifies its applicability.

Because total mesh stiffness of DDC or TDC models is affected by the dynamic mesh force, it can only be obtained jointly after calculating dynamic equations. Although dynamic mesh force fluctuates, individual tooth pair consistently sustains a large load in the whole operation process. Consequently, the mesh stiffness calculated under the dynamic mesh force is similar to the static result, as illustrated in Figure 4(b).

Under different crack severities, the minimum film thickness and friction coefficient of the cracked tooth pair are shown in Figure 5. In the first DTC region (corresponding to the root position for the cracked pinion), the minimum film thickness increases slightly with the crack severity, and friction coefficient reduces moderately. In the second DTC region (corresponding to the tip position for the cracked pinion), the minimum film thickness grows noticeably with the crack severity, whereas friction coefficient decreases gradually. In this region, bearing capacity of cracked tooth pair significantly decreases. In STC region, the minimum film thickness rises mildly due to the transient squeezing effect, whereas surface friction coefficient is basically the same because of constant tooth force.

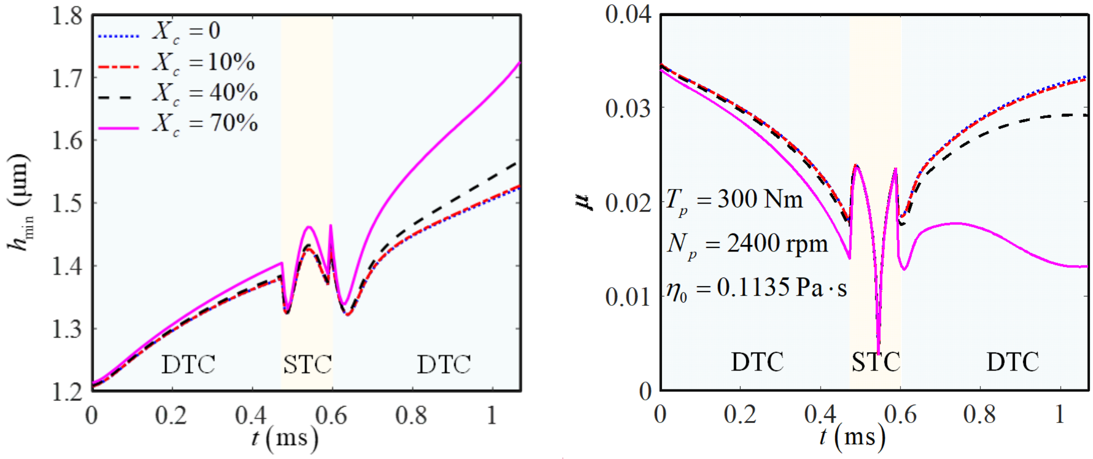

(a) Minimum film thickness (b) Friction coefficient

FIGURE 5. Lubrication performance for cracked tooth pair with different crack severities

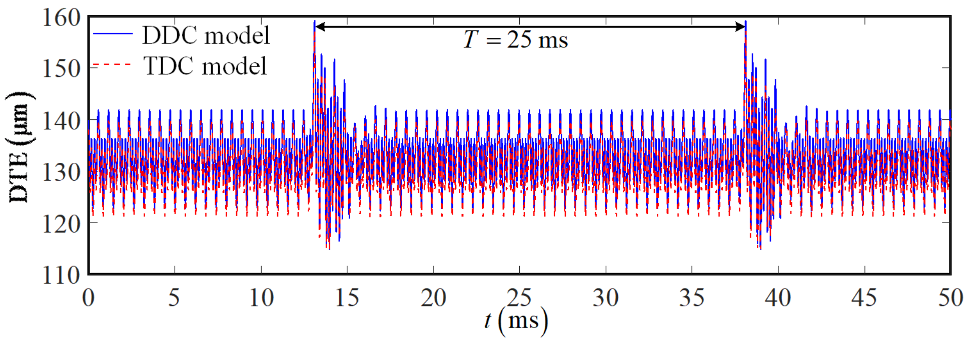

FIGURE 6. Time domain of DTE for a cracked gear pair ($X_c = 70\%$)

A cracked gear pair is used to simulate, which consists of a cracked pinion and a healthy gear. Time domains of the DTE are obtained from DDC model and TDC model, as shown in Figure 6. Under 70% crack severity degree, the peak-valley value of DTE predicted by DDC model is 44.29 μm. Similarly, this value from TDC model is 42.25 μm. Compared with DDC model, it is obvious that the time waveform from TDC model shows a downward trend. This observed behavior predominantly originates from two synergistic mechanisms. On the one hand, the film thickness is introduced between two meshing surfaces, which changes the actual value of backlash during operation process. On the other hand, oil film thickness leads to a reduction of the combined mesh stiffness of the gear pair, whereas its squeezing effect will restrain the vibration amplitude. Under the action of structural damping and lubrication effect, the vibration signal induced by root crack fault gradually weakens after several mesh cycles.

The frequency spectrograms obtained by two models are described in Figure 7(a) and Figure 8(a), and some amplitude components of mesh frequency, shaft frequency and other harmonic frequencies are listed. Under the lubrication effect, amplitudes of the first four order mesh frequency decrease to some extent.

Due to the emergence of tooth root crack, several frequency clusters appear near the resonance frequencies. The center of each spectral cluster exhibits precise alignment with fundamental resonance modes, whereby concomitant sideband structures emerge through parametric modulation, as shown in Figure 7(b) and Figure 8(b). For example, there

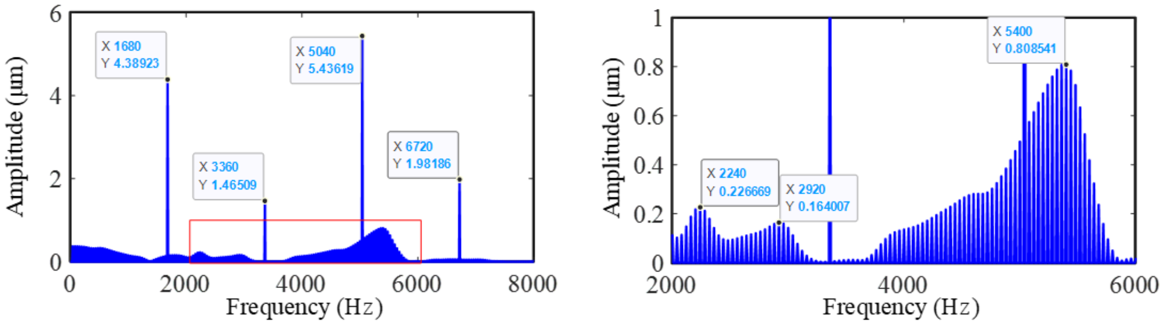

(a) Full-scale view (b) Zoomed-in view in $[2000, 6000]$ Hz

FIGURE 7. Frequency domain of the DTE from DDC model

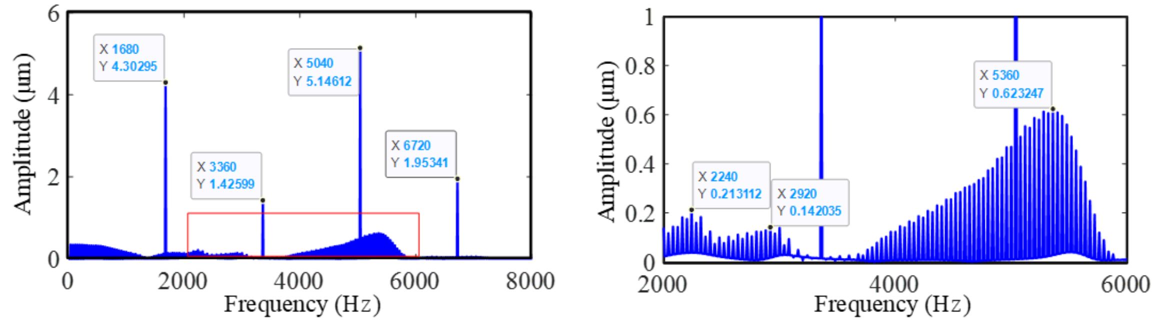

(a) Full-scale view (b) Zoomed-in view in $[2000, 6000]$ Hz

FIGURE 8. Frequency domain of the DTE from TDC model

is a distinct frequency cluster in the frequency range of $[4800, 5800]$ Hz, which consists of a set of spikes spaced at 40Hz. That is, the rotation frequency of the pinion, $n_p/60$. Some phenomena can be observed: 1) dynamic simulation of gear system considers the lubrication effect, and thus amplitudes of major frequencies decreases; 2) the peak of frequency cluster induced by root crack moves slightly backward, attributed to lubrication performance.

Considering system damping and oil film damping, there is a clear difference in amplitude between the two sides at the center of each spectral cluster. As described in [26], the amplitudes of those sidebands around the mesh frequency harmonics are asymmetrical, and the side close to the natural frequency would be higher than the other side. Therefore, the results of the proposed model maintain good consistency, regardless of the dry contact condition or lubrication condition.

To research the impact of lubrication performance on effectiveness of condition indicators, dynamic responses of the cracked gear pair are simulated under the above working condition. Figure 9 describes RMS and kurtosis values of DTE and translational displacement under dry and lubrication contact conditions. Magnitudes of RMS and kurtosis values increase with the tooth crack severity. Whereas, the kurtosis value is obviously greater than the RMS value, and the effectiveness of kurtosis is better when crack depth is greater.

Compared to the dry contact model, using the lubrication model results in a slight reduction in condition indicators for both dynamic transmission error and translational displacement along the LOA direction, as shown in Figures 9(a) and 9(c). Notably, RMS and kurtosis values associated with these two displacements demonstrate persistent

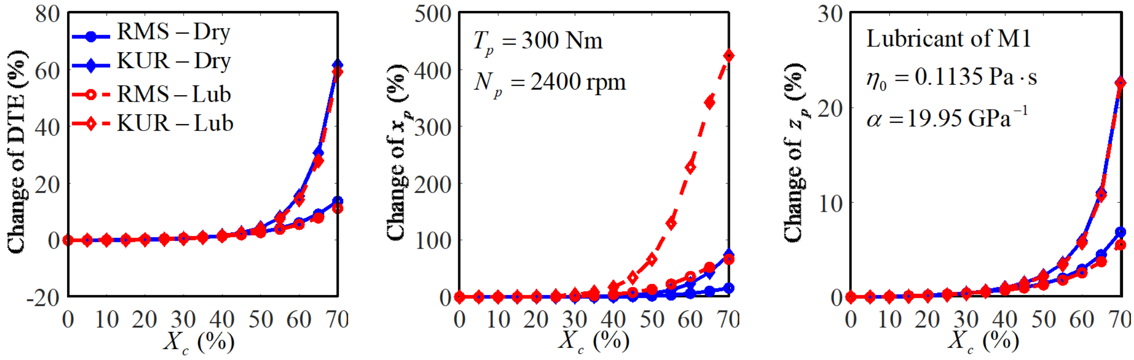

(a) DTE (b) x_p (c) z_p

FIGURE 9. Changes of RMS and kurtosis of vibration displacement versus crack severity

diagnostic efficacy, maintaining their effectiveness despite the nonlinear damping influences inherent in elastohydrodynamic lubrication regime at meshing interfaces. Because the support stiffness of bearings is two to three times larger than mesh stiffness of the gear pair, condition indicators of z_p are obviously smaller than that of the DTE.

Compared with DDC model, both RMS and kurtosis values of translational displacement increase along OLOA direction under lubrication effect, as illustrated in Figure 9(b). DDC model adopts a constant Coulomb friction coefficient for simulation ($\mu = 0.07$), which is not related to the growth of crack severity. Nevertheless, the TDC model accounts for the effect of crack fault on surface friction coefficient during operation process, leading to increased condition indicators of x_p.

With the increase of crack depth, the effect of crack failure on dynamic responses for the gear system becomes more and more serious. Therefore, crack severity propagation is determined by observing the distribution of frequency cluster and variation of condition indicators, so as to provide support for gear fault diagnosis in industrial systems.

5. **Conclusions.** Based on stiffness variation of cracked tooth pair during operation process, the load distribution factor considering a pinion tooth crack and lubrication effect is analyzed. Subsequently, the effect of root crack on lubrication performances is studied, and then the influence of crack fault on the tribo-dynamic characteristics of gear system is analyzed. The main conclusions are drawn as follows.

1) Compared with the healthy gear pair, tooth crack fault changes load distribution factor for the cracked gear pair, and then affects the oil film thickness and friction coefficient.

2) For the cracked gear pair, amplitudes of both the first four order harmonic frequencies and frequency cluster centers of the DTE are smaller than those under the dry contact condition, which suggests that lubrication effect suppresses dynamic responses.

3) Condition indicators demonstrate stable diagnostic capacity, even when considering both crack fault and lubrication performance. Condition indicators increase with crack severity, especially the kurtosis value. Additionally, the variation trend of those is more obvious in OLOA direction.

4) Future research will extend the proposed tribo-dynamic model to incorporate frictional thermal effects involving tooth surfaces, thereby providing more accurate support for fault diagnosis.

Acknowledgment. This work is partially supported by the Science and Technology Research Program of Chongqing Municipal Education Commission (Grant No. KJQN202200 843), the Doctoral Funding of Chongqing Technology and Business University, China (Grant No. 2256008).

REFERENCES

[1] Y. Luo, N. Baddour and M. Liang, Dynamical modeling and experimental validation for tooth pitting and spalling in spur gears, *Mechanical Systems and Signal Processing*, vol.119, pp.155-181, 2019.
[2] X. Liang, M. J. Zuo and Z. Feng, Dynamic modeling of gearbox faults: A review, *Mechanical Systems and Signal Processing*, vol.98, pp.852-876, 2018.
[3] T. Eritenel and R. G. Parker, An investigation of tooth mesh nonlinearity and partial contact loss in gear pairs using a lumped-parameter model, *Mechanism and Machine Theory*, vol.56, pp.28-51, 2012.
[4] A. Saxena, M. Chouksey and A. Parey, Effect of mesh stiffness of healthy and cracked gear tooth on modal and frequency response characteristics of geared rotor system, *Mechanism and Machine Theory*, vol.107, pp.261-273, 2017.
[5] S. Wu, M. J. Zuo and A. Parey, Simulation of spur gear dynamics and estimation of fault growth, *Journal of Sound and Vibration*, vol.317, nos.3-5, pp.608-624, 2008.
[6] Z. Chen and Y. Shao, Dynamic simulation of spur gear with tooth root crack propagating along tooth width and crack depth, *Engineering Failure Analysis*, vol.18, no.8, pp.2149-2164, 2011.
[7] Z. Chen, J. Zhang, W. Zhai, Y. Wang and J. Liu, Improved analytical methods for calculation of gear tooth fillet-foundation stiffness with tooth root crack, *Engineering Failure Analysis*, vol.82, pp.72-81, 2017.
[8] R. Ma and Y. Chen, Research on the dynamic mechanism of the gear system with local crack and spalling failure, *Engineering Failure Analysis*, vol.26, pp.12-20, 2012.
[9] Z. Meng, G. Shi and F. Wang, Vibration response and fault characteristics analysis of gear based on time-varying mesh stiffness, *Mechanism and Machine Theory*, vol.148, 103786, 2020.
[10] Z. Wan, H. Cao, Y. Zi, W. He and Z. He, An improved time-varying mesh stiffness algorithm and dynamic modeling of gear-rotor system with tooth root crack, *Engineering Failure Analysis*, vol.42, pp.157-177, 2014.
[11] S. He, S. Cho and R. Singh, Prediction of dynamic friction forces in spur gears using alternate sliding friction formulations, *Journal of Sound and Vibration*, vol.309, nos.3-5, pp.843-851, 2008.
[12] S. Li and A. Kahraman, A tribo-dynamic model of a spur gear pair, *Journal of Sound and Vibration*, vol.332, no.20, pp.4963-4978, 2013.
[13] C. Zhou and Z. Xiao, Stiffness and damping models for the oil film in line contact elastohydrodynamic lubrication and applications in the gear drive, *Applied Mathematical Modelling*, vol.61, pp.634-649, 2018.
[14] Z. Xiao, C. Zhou, S. Chen and Z. Li, Effects of oil film stiffness and damping on spur gear dynamics, *Nonlinear Dynamics*, vol.96, pp.145-159, 2019.
[15] C. Zhou, Y. Shen and Z. Wang, Research on vibration suppression of transmission chain in wind power generation system with gear clearance based on internal model control, *International Journal of Innovative Computing, Information and Control*, vol.18, no.4, pp.1247-1263, 2022.
[16] C. Zhou, Y. Shen and Y. Zhou, Research on vibration suppression of four-mass transmission chain in wind power generation system with gear clearance, *International Journal of Innovative Computing, Information and Control*, vol.20, no.3, pp.839-856, 2024.
[17] Z. Chen, Y. Jiang, S. Li, Z. Tong, S. Tong and N. Tang, Effect of lubricant viscosity on dynamics of high-precision gear considering lubricant-induced backlash reduction, *Tribology International*, vol.168, 107447, 2022.
[18] J. Zhao, L. Hou, Z. Li, H. Zhang and R. Zhu, Prediction of tribological and dynamical behaviors of spur gear pair considering tooth root crack, *Engineering Failure Analysis*, vol.135, 106145, 2022.
[19] X. Yang, E. Tofighi-Niaki, M. J. Zuo, Z. Tian, M. S. Safizadeh and D. Qin, Analysis of spur gearbox dynamics considering tooth lubrication and tooth crack severity progression, *Tribology International*, vol.178, 108027, 2023.
[20] Z. Cao, Z. Chen and H. Jiang, Nonlinear dynamics of a spur gear pair with force-dependent mesh stiffness, *Nonlinear Dynamics*, vol.99, no.2, pp.1-15, 2019.
[21] Z. Li, C. Zhu, H. Liu and Z. Gu, Mesh stiffness and nonlinear dynamic response of a spur gear pair considering tribo-dynamic effect, *Mechanism and Machine Theory*, vol.153, 103989, 2020.

[22] L. Wang et al., Effects of spalling fault on dynamic responses of gear system considering three-dimensional line contact elasto-hydrodynamic lubrication, *Engineering Failure Analysis*, vol.132, 105930, 2022.
[23] H. Ma, R. Song, X. Pang and B. Wen, Time-varying mesh stiffness calculation of cracked spur gears, *Engineering Failure Analysis*, vol.44, pp.179-194, 2014.
[24] W. Qin, J. Chao and L. Duan, Study on stiffness of elastohydrodynamic line contact, *Mechanism and Machine Theory*, vol.86, pp.36-47, 2015.
[25] P. Yang and S. Wen, A generalized Reynolds equation based on non-Newtonian flow in lubrication mechanics, *Acta Mechanica Sinica*, vol.6, no.4, pp.289-295, 1990.
[26] Y. Li, K. Ding, G. He and H. Lin, Vibration mechanisms of spur gear pair in healthy and fault states, *Mechanical Systems and Signal Processing*, vol.81, pp.183-201, 2016.

Author Biography

Zufeng Li received the bachelor's degree in Mechanical Engineering from Chongqing University, China, in 2013. He received the Ph.D. degree in School of Mechanical Engineering from Chongqing University, in 2020. From 2021 until now, he is a research assistant in Chongqing Technology and Business University, China. His current research interests include the transmission system dynamics, failure diagnosis and nonlinear control theory.

Jiarui Fan is a postgraduate student in School of Mechanical Engineering at Chongqing Technology and Business University, China. He received a bachelor's degree from Jianghan University, China, in June 2024. His research focuses on the dynamic characteristics analysis of system and robot application.